Journal of Experimental Botany, Vol. 64, No. 4, pp. 1121–1134, 2013
doi:10.1093/jxb/ert006
This paper is available online free of all access charges (see http://jxb.oxfordjournals.org/open_access.html for further details)

Journal of Experimental Botany
www.jxb.oxfordjournals.org

RESEARCH PAPER

Protein tyrosine nitration in pea roots during development and senescence

Juan C. Begara-Morales[2], Mounira Chaki[1], Beatriz Sánchez-Calvo[2], Capilla Mata-Pérez[2], Marina Leterrier[1], José M. Palma[1], Juan B. Barroso[2] and Francisco J. Corpas[1,*]

[1] Department of Biochemistry, Molecular and Cellular Biology of Plants, Estación Experimental del Zaidín (EEZ), Consejo Superior de Investigaciones Científicas, E-18080 Granada, Spain
[2] Group of Molecular Signaling and Antioxidant Systems in Plants, Associated Unit to Consejo Superior de Investigaciones Científicas (EEZ), Area of Biochemistry and Molecular Biology, University of Jaen, E-23071 Jaén, Spain

* To whom correspondence should be addressed. E-mail: javier.corpas@eez.csic.es

Received 26 November 2012; Revised 2 January 2013; Accepted 2 January 2013

Abstract

Protein tyrosine nitration is a post-translational modification mediated by reactive nitrogen species (RNS) that is associated with nitro-oxidative damage. No information about this process is available in relation to higher plants during development and senescence. Using pea plants at different developmental stages (ranging from 8 to 71 days), tyrosine nitration in the main organs (roots, stems, leaves, flowers, and fruits) was analysed using immunological and proteomic approaches. In the roots of 71-day-old senescent plants, nitroproteome analysis enabled the identification a total of 16 nitrotyrosine-immunopositive proteins. Among the proteins identified, NADP-isocitrate dehydrogenase (ICDH), an enzyme involved in the carbon and nitrogen metabolism, redox regulation, and responses to oxidative stress, was selected to evaluate the effect of nitration. NADP-ICDH activity fell by 75% during senescence. Analysis showed that peroxynitrite inhibits recombinant cytosolic NADP-ICDH activity through a process of nitration. Of the 12 tyrosines present in this enzyme, mass spectrometric analysis of nitrated recombinant cytosolic NADP-ICDH enabled this study to identify the Tyr392 as exclusively nitrated by peroxynitrite. The data as a whole reveal that protein tyrosine nitration is a nitric oxide-derived PTM prevalent throughout root development and intensifies during senescence.

Key words: Nitration, nitric oxide, nitrotyrosine, peroxynitrite, plant development, reactive nitrogen species, senescence.

Introduction

Nitric oxide (NO) and related molecules such as *S*-nitrosoglutathione (GSNO) and peroxynitrite ($ONOO^-$) belong to the group of compounds called reactive nitrogen species (RNS). Although the metabolism of RNS and their physiological implications have been intensively studied in relation to animal cells, less is known about plant cells. RNS can mediate post-translational modifications (PTMs) of proteins which could be pathological processes and/or mechanisms of cellular signalling (Radi, 2004; Dalle-Donne *et al.*, 2005; Ischiropoulos and Gow, 2005; Corpas *et al.*, 2007, 2009). These PTMs mediated by RNS include processes like binding to metal centres, nitrosylation of thiol and amine groups, and nitration of tyrosine and other amino acids (Gow *et al.*, 2004). Nitrosylation of thiols to produce *S*-nitrosothiols and nitration of tyrosine residues in order to produce 3-nitrotyosine (NO_2-Ty) have been the subject of considerable study in relation to animal cells as they appear to be involved in signalling processes.

Protein tyrosine nitration is a covalent protein modification resulting from the addition of a nitro ($-NO_2$) group to one of two equivalent ortho carbons in the aromatic ring of tyrosine residues (Gow *et al.*, 2004). This process has routinely been used as a marker of pathological disease and oxidative stress in animal cells (Ischiropoulos, 2003). However,

tyrosine nitration of protein residues can alter protein function because the incorporation of large groups onto the aromatic ring lowers the pKa of the phenolic group and causes both steric and electronic perturbations that affect tyrosine's capacity to function in electron-transfer reactions and to maintain protein conformation (Eiserich *et al.*, 1999). Thus, tyrosine nitration has been reported to lead to either gain or loss of function (Greenacre and Ischiropoulos, 2001; Radi, 2004). This NO-mediated PTM has also been studied in plants under stress conditions and has been proposed as a potential nitrosative stress marker (Corpas *et al.*, 2007, 2013). A rise in protein tyrosine nitration has therefore been reported under biotic (Chaki *et al.*, 2009) and abiotic stresses that include salinity (Valderrama *et al.*, 2007; Corpas *et al.*, 2009; Tanou *et al.*, 2012), extreme temperature (Chaki *et al.*, 2011; Airaki *et al.*, 2012), and arsenic (Leterrier *et al.*, 2012a).

However, not much information is available on protein tyrosine nitration during development and senescence in relation to higher plants. In this study, the protein profile of tyrosine nitration in the main organs of pea plants was studied. In addition, after studying the nitroproteome of senescent roots, this work discovered that cytosolic NADP-isocitrate dehydrogenase (ICDH) is a molecular target of this NO-mediated PTM which provoked its inhibition.

Materials and methods

Plant materials and growth conditions

Pea (*Pisum sativum* L., cv Lincoln) seeds, obtained from Royal Sluis (Enkhuizen, Holland), were germinated in vermiculite under optimum conditions (14/7 h 21/18 °C light/dark cycle, 190 µE m^{-2} s^{-1}, 50–60% relative humidity). For senescence, pea seedlings of 14 days were transferred and then grown in aerated optimum nutrient solutions under greenhouse conditions (28/18 °C light/dark temperature; 80% relative humidity) for a total time of 71 days. Samples of roots, stems, and leaves were taken at 8, 12, 14, 16, and 71 days. Flowers and whole fruits were taken from plants aged 71 days.

Crude extracts of plant tissues

Tissues were frozen in liquid N_2 and ground in a mortar with a pestle. The powder was suspended in a homogenizing medium containing 100 mM TRIS-HCl buffer (pH 8.0), 1 mM EDTA, 0.2 mM CHAPS, and 1 mM PMSF (1:2, w/v). Homogenates were centrifuged at 21,000 *g* for 20 min, and the supernatants were passed through Sephadex G-25 desalting columns (NP-10, Amersham) which eliminated low-molecular-weight substances (Mr <1000). The different flow-throughs were used for the assays.

Non-denaturing PAGE and detection of superoxide dismutase isoforms

Superoxide dismutase (SOD) isozymes were separated by native PAGE on 10% acrylamide gels and visualized by a photochemical method (Beauchamp and Fridovich, 1971). To identify the type of SOD isozyme, gels were preincubated separately at 25 °C for 30–45 min in 50 mM K-phosphate (pH 7.8), in the presence or absence of either 5 mM KCN or 5 mM H_2O_2 (Corpas *et al.*, 1998).

SDS-PAGE and Western blot

SDS-PAGE was done on 10% polyacrylamide gels as described by Laemmli (1970). Gels were stained with silver nitrate (Corpas and Trelease, 1998). For Western blot analysis, proteins were electroblotted to PVDF membranes by a semi-dry Trans-Blot cell (Bio-Rad). After transfer, membranes were used for cross-reactivity assays using polyclonal antibodies against nitrotyrosine (1:8000 dilution) (Chaki *et al.*, 2009), spinach cytosolic CuZnSOD (1:3000 dilution) (Kanematsu and Asada, 1989), and pea MnSOD (1:2000 dilution) (Corpas *et al.*, 2006b). For immunodetection, an affinity-purified goat anti-rabbit IgG–horseradish peroxidase conjugate (BioRad) and an enhanced chemiluminescence kit (ECLPLUS, Amersham) was used. As positive control, commercial nitrated BSA (Sigma) was used. Immunoblot experiments were performed a minimum of three times, with similar results. Protein concentration was determined with the Bio-Rad Protein Assay (Hercules, CA, USA), using BSA as a standard.

Detection of nitric oxide and peroxynitrite

Nitric oxide was detected with 10 µM 4,5-diaminoflorescein diacetate (DAF-FM-DA, Calbiochem) prepared in 10 mM TRIS-HCl (pH 7.4). Root cross-sections were incubated at 25°C for 1 h, in darkness, according to Corpas *et al.* (2006a). After incubation, samples were washed twice in the same buffer for 15 min each. Then root sections were embedded in a mixture of 15% acrylamide/bisacrylamide stock solution as described elsewhere (Corpas *et al.*, 2006a), and 80–100 µm-thick sections, as indicated by the vibratome scale, were cut under 10 mM phosphate-buffered saline (PBS). Sections were then soaked in glycerol/PBS containing azide (1:1, v/v) and mounted in the same medium for examination by confocal laser scanning microscopy (CLSM, Leica TCS SL), using standard filters and collection modalities for DAF-2 green fluorescence (excitation 495 nm; emission 515 nm). Background staining, routinely negligible, was controlled with root sections unstained. As control, sections were preincubated 30 min at 25 °C with 200 µM 2-(4-carboxyphenyl)-4,4,5,5-tetramethylimidazoline-1-oxyl-3-oxide, an NO scavenger.

Peroxynitrite was detected using the fluorescent reagent 3'-(*p*-aminophenyl) fluorescein (APF, Invitrogen) (Chaki *et al.*, 2009). Pea root sections were incubated at 25 °C for 1 h, in darkness, with 10 µM APF prepared in 10 mM TRIS-HCl (pH 7.4) and were processed as described by Chaki *et al.* (2009). Then, the samples were washed twice in the same buffer for 15 min each and mounted in a microscope slide for examination by CLSM using standard filters and collection modalities for APF green fluorescence (excitation 495 nm; emission 515 nm).

Immunolocalization of nitrotyrosine

Pea roots were cut into 4–5 mm pieces and fixed in 4% (w/v) *p*-formaldehyde in 0.1 M phosphate buffer (PB, pH 7.4) for 3 h at room temperature. Then they were cryoprotected by immersion in 30% (w/v) sucrose in PB overnight at 4 °C. Serial sections, 60-µm thick, were obtained by means of a cryostat (2800 Frigocut E, Reichert-Jung, Vienna, Austria). The sections were incubated with a rabbit polyclonal antibody against 3-nitrotyrosine (NO_2-Tyr) diluted 1:300 in TBSA-BSAT (5 mM TRIS buffer pH 7.2, 0.9% (w/v) NaCl containing 0.05% (w/v) sodium azide, 0.1% (w/v) BSA, 0.1% (v/v) Triton X-100) for 3 days at 4 °C. After several washes, sections were incubated with Cy3-labelled anti-rabbit IgG (Amersham) diluted 1:1000 in TBSA-BSAT, for 1 h at room temperature, and then mounted in PBS/glycerol (1:1). Controls for background staining, which was usually negligible, were performed by replacing the corresponding primary antiserum by preimmune serum. Root sections were examined by CLSM using standard filters for Cy2-streptavidin (excitation 492 nm; emission, 510 nm) and Cy3-labelled anti-rabbit IgG (excitation 550 nm; emission, 570 nm).

Protein concentration of pea roots, 2D gel electrophoresis, and immunoblot analysis

Pea roots from 71-day-old plants were washed four times with tap water and twice with distilled water and drying with paper towel.

Tissues (45 g) were frozen in liquid N_2 and ground in a mortar with a pestle. The powder was suspended in 125 ml of 50 mM HEPES (pH 7.6). The homogenate was filtered through four layers of nylon and centrifuged at 20,000 *g* for 15 min. To achieve the protein precipitation, three volumes of 100% acetone at –20 °C was added to the supernatants with stirring for 30 min (70% final concentration, v/v) and the mixture was centrifuged at 16,000 *g* for 15 min The precipitate, which contained most of the proteins, was taken up in 5 ml of 50 mM HEPES and incubated overnight at 4 °C with agitation. Then, it was centrifuged at 39,000 *g* for 20 min. The supernatants were passed through Sephadex G-25 gel filtration columns (NAP-10, Amersham) which were equilibrated and eluted with 50 mM HEPES. The final concentration of the protein extract was 0.88 µg $µl^{-1}$ in 7 ml final volume (6 mg total yield).

Proteins were separated by two-dimensional gel electrophoresis (2-DE). Isoelectric focusing was carried out with precast IPG-gels pH 3–10. Each gel was loaded with 150 µg protein. The second-dimension separation was performed by glycine SDS-PAGE according to Laemmli (1970). Gels were SYPRO Ruby stained, scanned, and analysed with Bio-Rad PDQuest software. Western blot of the 2D gel was performed as described above with a minimum of three replicates with similar results, and then the immunoblot probed with a polyclonal antibody against nitrotyrosine (1:8000 dilution).

In situ digestion of 2D spots and protein identification by MALDI TOF/TOF analysis

Identified spots in the gel were automatically recovered using Investigator ProPic Protein Picking Workstation (Genomic Solutions). Then, they were digested with trypsin using an Investigator ProGest Protein Digestion Station (Genomics Solutions). Briefly the procedure was as follow: destaining with 40% acetonitrile/200 mM NH_4HCO_3; for 30 min (twice); wash with 25 mM NH_4HCO_3 for 5 min and 25 mM NH_4HCO_3/50% acetonitrile for 15 min, respectively (twice). Then, samples were dehydrated with 100% acetonitrile for 5 min and dried up. The samples were hydrated with 10 µl trypsin in 25 mM NH_4HCO_3 (12.5 ng $µl^{-1}$) at room temperature for 10 min then digested at 37 °C for 12 h. The reaction was stopped by adding 10 µl of 0.5% trifluoroacetic acid (TFA). Peptides were purified using a ProMS station (Genomic Solutions) using a column C18 (ZipTip, Millipore) eluted with α-cyano-4-hydroxycinnamic acid (3 mg ml^{-1}) in 70% acetonitrile/0.1% TFA) in a MALDI plate (1 µl). After crystallization the samples were analysed by MALDI TOF/TOF mass spectrometry in a range mass-to-charge ratio (m/z) of 800–4000 Da using a spectrometer (4700 Proteomics Analyzer, Applied Biosystems) in automatic mode. Internal calibration of the mass spectrums were done using the m/z of the peptides from porcine trypsin autolysis (mass MH^+ 842.509 and 2211.104), given a precision in the m/z ratio of 20 ppm. From each samples were selected the three spectrums with the higher m/z ratio. The protein identification was done by combining the MS spectrum with the corresponding MS/MS using MASCOT program in the database of MatrixScience (http://www.matrixscience.com). The following search parameters were applied limiting the taxonomic category to plants; a mass tolerance of 100 ppm and one incomplete cleavage were allowed; complete alkylation of cysteine by carbamidomethylation and partial oxidation of methionine.

Expression and purification of recombinant cytosolic NADP-ICDH from pea

cDNA encoding mature cytosolic NADP-ICDH (AY509880) was amplified by PCR from the first-strand cDNA synthesized from total RNA of pea using the Fast Start High Fidelity polymerase (Roche) and the specific primer set 5'-CTCGAGCATGGCATTC CAGAAAATCAAAG-3' and 5'-TCTGCAGTCACAAATCTACG CAGAGATCTTCG-3'. Amplfication products (1261 bp) were detected by electrophoresis in 1% (w/v) agarose gels stained with ethidium bromide, and the visualized band was cut and extracted from the gel (High Pure PCR Product Purification kit, Roche). The purified fragments were cloned into the pGEM-T Easy vector (Promega). The positive clones were confirmed by sequencing. Then, they were subcloned by prior digestion with *Bam*HI and *Xho*I into the pALEXb vector. Recombinant protein carrying a N-terminal choline-binding domain was produced using *Escherichia coli* strain BIVU0811, which was routinely cultured overnight at 37 °C in LB medium with kanamicin (25 mg l^{-1}) and ampicillin (100 mg l^{-1}). Gene expression was induced by the addition of 1 mM salicylate and 10 mM 3-methyl benzoate in 250 ml and culture at 20 °C overnight to provide a higher proportion of soluble protein. Cells were harvested by centrifugation and resuspended in 20 ml of PBS buffer (pH 7.0) containing 25 U ml^{-1} DNAse I and 10 mM $MgCl_2$ and commercial protease inhibitor (Complete, Roche). Cells were lysed with a Niro Soavi NS1001L Panda High-Pressure homogenizer at a pressure of 800–900 bar. Then, the cell lysate was centrifuged at 10,000 *g* at 4 °C for 15 min and the supernatant was used for purification of recombinant protein using a 1-ml LYTRAP column (BIOMEDAL). The column was washed with 20 ml of 20 mM K-phosphate buffer (pH 7.0) containing 300 mM NaCl and 5 mM choline. The protein was eluted in 1-ml fractions using a discontinuous gradient of choline prepared in the same buffer with 100 mM NaCl and 20 mM choline (fraction E1), 50 mM choline (E2), 75 mM choline (E3), 100 mM choline (E4), 150 mM choline (E5), 200 mM choline (E6), and 250 mM choline (E7). The samples were analysed by 10% SDS-PAGE and stained with Coomassie blue.

Catalase and NADP-ICDH activity assay: treatment with SIN-1 (peroxynitrite donor)

Catalase activity was determined by measuring the disappearance of H_2O_2, as described by Aebi (1984). NADP-ICDH activity was determined spectrophotometrically by recording the reduction of NADP at 340 nm (Leterrier *et al.*, 2007). The molecule SIN-1 (3-morpholinosydnonimine) has been demonstrated to generate peroxynitrite being a protein-nitrating compound (Daiber *et al.*, 2004). Recombinant NAPD-ICDH was incubated at 37 °C for 1 h with increased concentrations (0–5 mM) of SIN-1 (Calbiochem) made up fresh before use. Then, the samples were passed through NAP-10 column to avoid any interference of SIN-1 with the activity assay. Protein concentration was determined with the Bio-Rad Protein Assay, using BSA as standard. Nitration was corroborated by immunoblot using a polyclonal antibody against NO_2-Tyr (Chaki *et al.*, 2009).

Identification of nitrated tyrosine in recombinant cytosolic NADP-ICDH LC-MS/MS

Purified cytosolic NADP-ICDH was processed with a protocol which involved reduction with dithiothreitol (DTT), derivatization with iodoacetamide (IAA), and enzymic digestion with trypsin (37 °C, 8 h). The sample was purified using solid-phase extraction cartridges to eliminate choline interferences. The resulting peptide mixture was analysed using a MALDI-TOF/TOF mass spectrometer (4800, AB Sciex) to evaluate the quality of the sample. MALDI-TOF spectra were interpreted using a peptide mass fingerprinting database search (Protein Prospector program). The database used for identification was Uniprot (release 2011_02). Then, sample was analysed by LC-MS/MS using a Velos-LTQ mass spectrometer equipped with a microESI ion source (ThermoFisher, San Jose, CA, USA). The sample was evaporated to dryness and diluted up to 40 µl with water containing 5% methanol and 1% formic acid. Then, the sample was loaded in a chromatographic system consisting in a C18 preconcentration cartridge (Agilent Technologies, Santa Clara, CA, USA) connected to a 10 cm long, 150 µm i.d. C18 column (Vydac, IL, USA). The separation was done at 1 µl min^{-1} in a 30 min acetonitrile gradient from 3 to 40% (solvent A 0.1% formic acid; solvent B acetonitrile/0.1% formic acid). The HPLC system was composed by an Agilent 1200 capillary pump, binary pump, a thermostated

microinjector, and a micro-switch valve. The Velos-LTQ instrument was operated in the positive ion mode with a spray voltage of 2 kV. The scan range of each full MS was m/z 400–2000. After each MS scan, a collection of targeted MS/MS spectra were obtained in order to identify both the unmodified and nitrated form of the expected tyrosine-containing peptides. The parent mass list of the targeted scan was selected to ensure maximum coverage of the tyrosine-containing tryptic peptides for NADP-ICDH. The list of targeted m/z values was obtained after *in silico* digestion of the proteins using nitrated tyrosine as a dynamic modification. The resulting list of predicted peptides (including both the nitrated and the unmodified forms) was filtered to exclude all peptides that did not contain tyrosine residues.

MS/MS spectra were searched using Proteome Discoverer software (ThermoFisher,) with the following parameters: peptide mass tolerance 2 Da, fragment tolerance 0.8 Da, enzyme set as trypsin, and no missed cleavages. Dynamic modifications were cysteine carbamidomethylation (+57 Da), methionine oxidation (+16 Da), and tyrosine nitration (+45 Da). The searches were performed using a database containing all the proteins listed in Supplementary Table S1 (available at *JXB* online). Identifications were filtered with XCorr > 3, P(pep) < 15%. The MS/MS spectrum of the nitrated tyrosine was manually validated by comparison of the spectra obtained for the unmodified peptide and the nitrated peptide.

Structural analysis of cytosolic NADP-ICDH

The 3D structure of pea NADP-ICDH was modelled using the structure of the pig NADP-ICDH (PDB code access 1lwd_B) at a resolution of 1.85 Å and a homology of 69.3%. The analysis of the quality of the model resulted in a 93.1% residue with a 3D-1D average score higher than 0.2 and 87.7% in the Ramachandran plot. Determining the sites important for the structure and/or function of the protein was performed using the database available at www.uniprot.org and by homology with the structure of the pig NADP-ICDH (Ceccarelli *et al.*, 2002). Next, this study performed a sequence alignment of pea ICDH (AAS49171.1), rice (AAU44104.1), *Arabidopsis* (AEE330821.1), human (O75874.2), and pork (1lwd_B). In this way, it was determined that residues with significant relevance in the structure and/or function of the NADP-ICDH that were conserved in various species (Huang and Colman, 2005) and therefore can have a similar function in the pea ICDH. The location of these zones, together with the Tyr392 nitration identified as target, within the structure of the protein was done using the program Rasmol.

Statistical analysis

To estimate the statistical significance between means, the data were analysed by Student's t-test.

Results

Fig. 1 shows the protein patterns analysed using silver stains and the corresponding tyrosine nitration protein patterns detected with an antibody against nitrotyrosine during development and senescence in the different pea organs of 8, 12, 14, and 16-day-old (young) and 71-day-old (senescent) plants (Pastori and del Río, 1997; Corpas *et al.*, 1999, 2004). In roots (Fig. 1A), the silver stain showed a general increase in the intensity of polypeptides, which reached very high levels in senescent plants (71 days old). On the other hand, roots showed a similar protein tyrosine nitration pattern in relation to all ages, with protein bands of 45, 52, 63, and 76 kDa, although its intensity increased with plant age and reached higher levels during senescence. There was also an additional

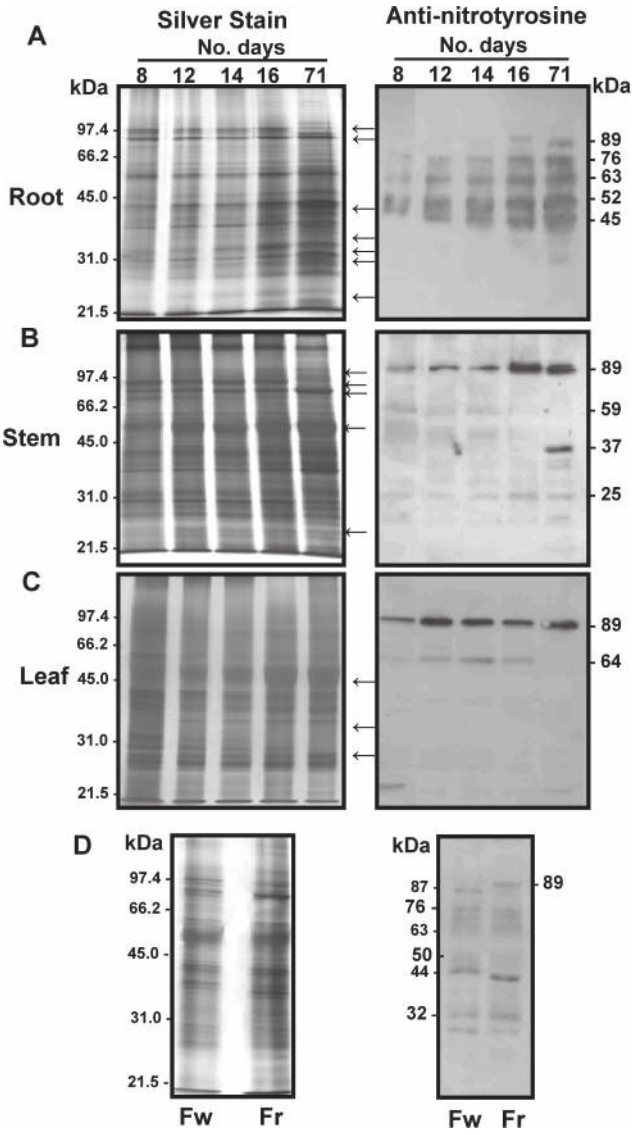

Fig. 1. Protein and tyrosine nitration pattern in organs of pea plants during natural development (8–16-days-old) and senescence (71-days-old). Silver-stained SDS gels (10%) and Western blots probed with a rabbit anti-nitrotyrosine polyclonal antibody at a 1:8000 dilution. (A) Root samples of pea plants aged 8–71 days (5 μg per lane); (B) stem samples of pea plants aged 8–71 days (10 μg per lane); (C) leaf samples of pea plants aged 8–71 days (20 μg per lane); (D) flowers (Fw) and fruits (Fr) of pea plants aged 71 days (10 μg per lane). Arrows indicate bands that have changed their intensity, disappeared, or become visible.

band of 89 kDa which appeared to become tyrosine nitrated after 16 days and became more intense during senescence. In stems (Fig. 1B), the silver stain protein pattern was different to that found in the other organs. The nitration profile was also different, with the most prominent band being 89 kDa, with other less intense bands (25 and 59 kDa) being detected. Moreover, during senescence, a new and very clear protein band of 37 kDa appeared. In leaves (Fig. 1C), the most visible band was 89 kDa, with a 64 kDa nitrated protein becoming more intense at day 14, which, however, disappeared in

senescent 71-day-old leaves. In the case of flowers and whole fruits, the silver and nitration patterns were also different from the other organs.

As roots had the clearest intensification profile for protein nitration, these organs were selected as subjects of further research. Previous studies have shown that, during senescence, there is an increase in ROS generation and an induction of antioxidative enzymes such as SODs in leaves (Pastori and del Río, 1997). SOD activity and protein content were thus analysed to determine whether there is a similar behaviour pattern during root development and senescence (Fig. 2). In roots, three SOD isozymes were detected, one MnSOD and two CuZnSODs (I and II, in order of their electrophoretic mobility in the non-denaturing gel). Fig. 2A shows that the MnSOD and CuZnSODs increased during development, with the increase being more evident in 71-day-old plants. Moreover, these increases in SOD activities were accompanied by an enhancement in the protein content of MnSOD and both CuZnSODs (Fig. 2B and C).

Content and cellular localization of NO, ONOO⁻, and tyrosine nitration in young and senescent roots

This work studied the content and localization of NO, $ONOO^-$, and tyrosine nitration in root cross-sections of 8-day-old (Fig. 3A, C, and E) and 71-day-old (Fig. 3B, D,

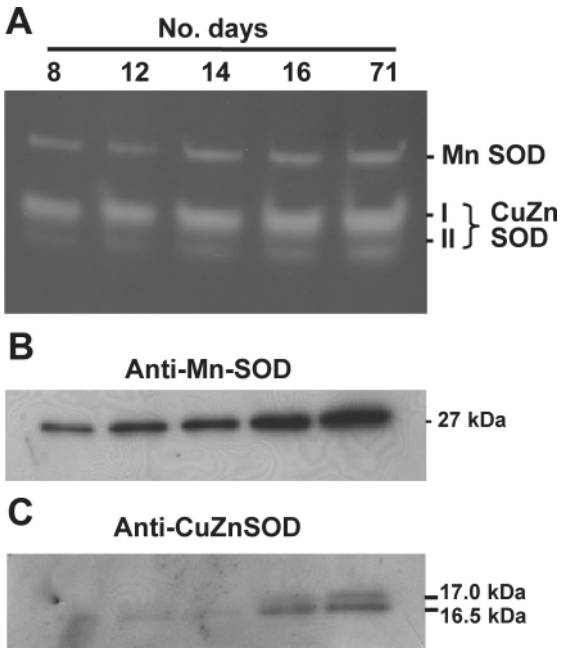

Fig. 2. Analysis of superoxide dismutase (SOD) isozymes present in roots of pea plants during natural development (8–16 days) and senescence (71 days). (A) Activity of SOD isozymes; SODs were separated by native PAGE on 10% (w/v) polyacrylamide gels, and gels were stained by the photochemical nitroblue tetrazolium method. (B and C) Western blot of pea root samples probed with antibodies against pea MnSOD (1:2000 dilution) and *Equisetum* CuZnSOD (1:3000 dilution), respectively. Proteins (8 μg per lane) were separated by 12% SDS-PAGE and transferred onto a PVDF membrane.

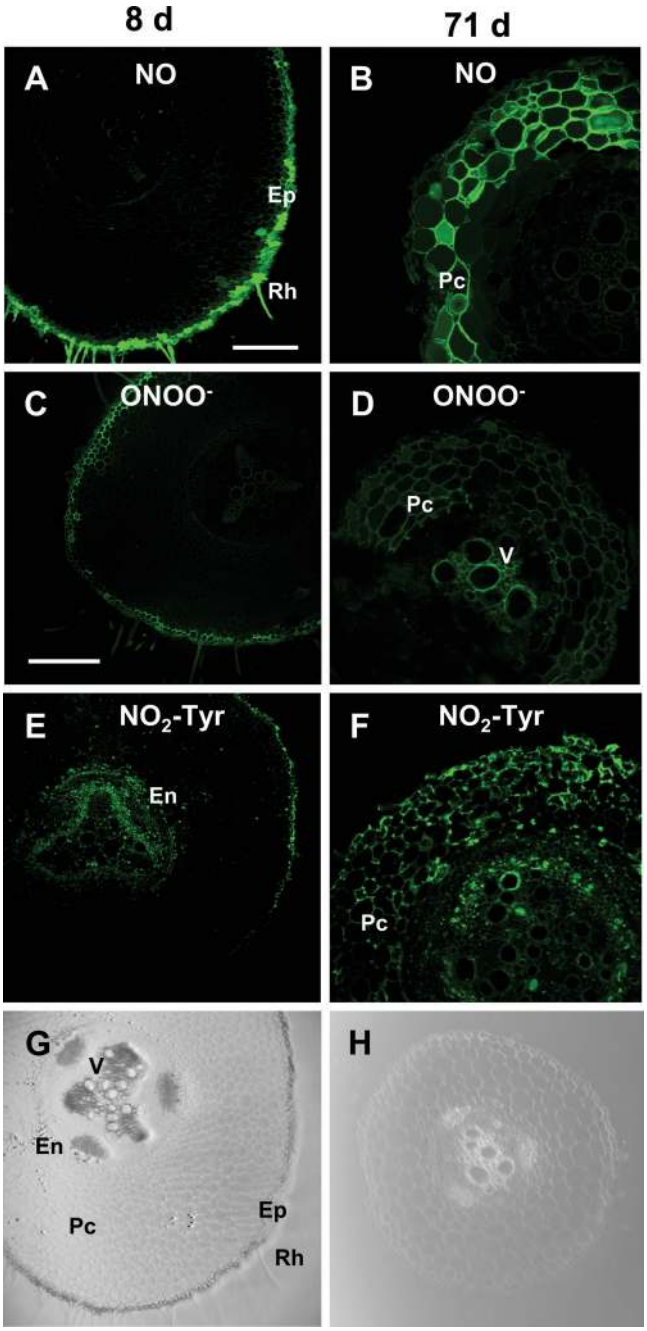

Fig. 3. Representative images illustrating confocal laser scanning microscopic detection of nitric oxide (NO), peroxynitrite ($ONOO^-$), and protein 3-nitrotyrosine (NO_2-Tyr) in root cross-sections of pea plants aged 8 and 71 days. (A–F) Cross-sections of pea roots (100 μm thick) were incubated with 10 μM 4,5-diaminoflorescein diacetate to detect NO (A and B), with 10 μM 3'-(*p*-aminophenyl) fluorescein to detect $ONOO^-$ (C and D), and with a specific antibody against NO_2-Tyr (E and F). (G and H) show representative bright-field image of the corresponding samples. The bright-green fluorescence corresponds to the detection of $^{\cdot}NO$, $ONOO^-$, or NO_2-Tyr in the corresponding panels. En, Endodermis; Ep, epidermis; Pc, parenchyma cells of the cortex; Rh, root hairs; V, vascular tissues. Bar = 300 μm (this figure is available in colour at *JXB* online).

and F) pea plants. In young roots, an intense green fluorescence due to NO was observed in the epidermal cells and root hairs. In senescent roots, NO extended to some cortex cell layers closer to the epidermis. In the case of $ONOO^-$, although localization in young roots was similar to that observed for NO, in senescent roots localization was also observed in vascular tissues. In the case of tyrosine nitration, the differences between young and senescent roots were greatest, as tyrosine nitration in senescent roots showed considerable intensification and a wide distribution in all cell types (epidermis, cortex, and vascular tissues).

Proteomic identification of tyrosine-nitrated proteins in roots of senescent 71-day-old pea plants

Fig. 4A shows the protein staining in a 2D gel of root samples from senescent pea plants and the corresponding immunoblot probed with an antibody against NO_2-Tyr. A total of 16 immunoreactive spots were detected. Fig. 4B shows zoom boxes to illustrate in more detail which immunoreactive spots were more intense. All 16 of these spots were analysed by MALDI-TOF mass spectrometry after tryptic digestion using the MASCOT search engine to analyse MS data in order to identify proteins from primary-sequence databases (Perkins *et al.*, 1999). The immunoreactive proteins identified are listed in Table 1, with the protein score confidence interval (CI) in almost all cases being over 99%, indicating that the proteins were not identified by random matches of peptide-mass data.

To gain a deeper understanding of the physiological importance of nitration in roots, the NADP-dependent isocitrate dehydrogenase (NADP-ICDH) was selected from among the proteins identified. NADP-ICDH, with a protein score CI of 100%, is an enzyme involved in cycling, redistribution, and export of amino acids, in addition to its primary function of GS/GOGAT-dependent nitrogen assimilation. NADP-ICDH also has the capacity to generate NAPDH which is essential for redox regulation and responding to oxidative stress (Valderrama *et al.*, 2006; Leterrier *et al.*, 2007, 2012a,b,c).

Expression and purification of cytosolic NADP-ICDH: effect of $ONOO^-$

As a means of increasing knowledge of pea NADP-ICDH's regulation mechanism, the recombinant protein was obtained by sequencing the pea clone and overexpression in *E. coli*. Fig. 5A shows 10% SDS-PAGE analysis of the different

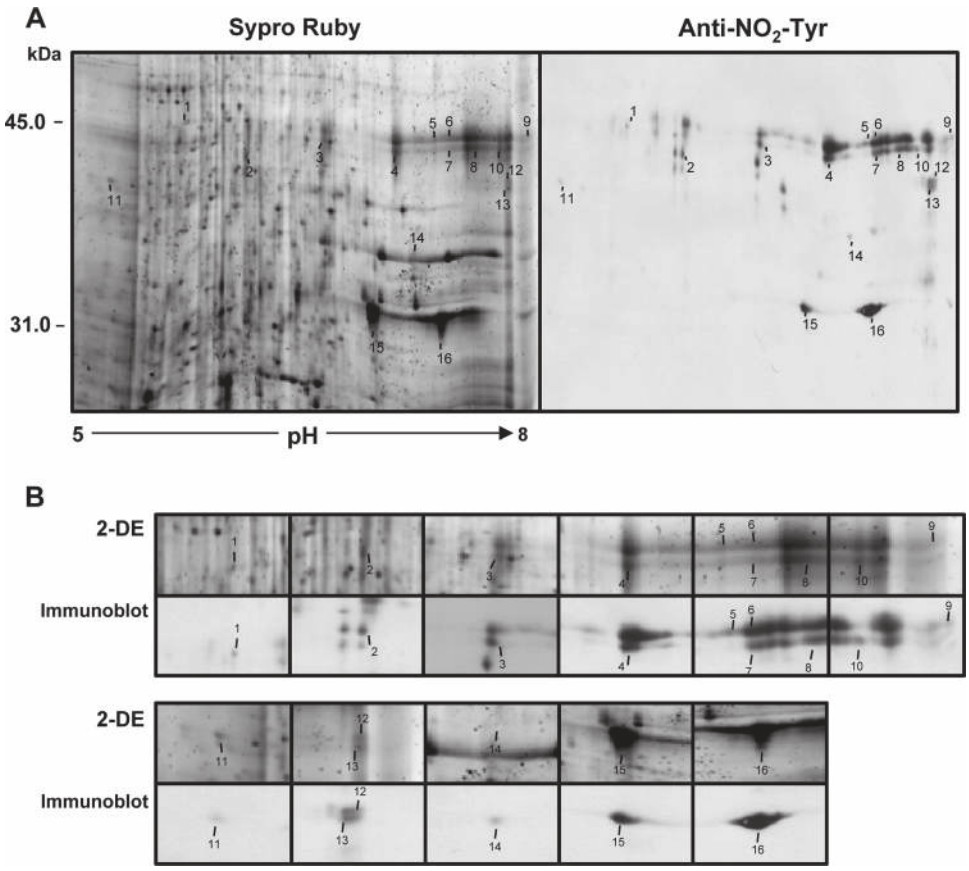

Fig. 4. Detection of nitrated proteins in roots of senescent pea plants by 2D electrophoresis and immunoblot. (A) Representative 2D electrophoresis (pH 5–8 for the first dimension) of pea root samples stained with Sypro Ruby and its corresponding immunoblot probed with a polyclonal antibody against nitrotyrosine (1:8000 dilution). Molecular-mass standards are indicated on the left in kDa. Approximately 150 μg protein was loaded per gel. Arrows indicate all the immunoreactive spots, and the numbers refer to the proteins listed in Table 1. (B) Zoom boxes illustrate details of immunoreactive spots.

Table 1. Identified 3-nitrotyrosine proteins from pea roots of senescence plants. Concentrated pea root extracts were subjected to 2D electrophoresis and immunoblot probed with an antibody against 3-nitrotyrosine. The identified spots were analysed by MALDI-TOF mass spectrometry after trypsin digestion. The MASCOT search engine was used to parse MS data in order to identify proteins from primary sequence databases. A protein score confidence interval (CI) close to 100% indicates that the protein is most likely correctly matched. MW, molecular weight; pI, isoelectric point.

Spot no.	Identified protein	Acc. no.	Protein score%CI (no. of identified peptides)	MW (pI)	Functional grouping
1	Predicted protein *Physcomitrella patens* subsp. *patens*	gi|168066110	71.035 (9)	41562.5 (5.24)	Pepsin-like aspartate protease
2	Amidase, hydantoinase/carbamoylase family protein, expressed *Oryza sativa* Japonica group	gi|108862917	98.676 (10)	40295.7 (5.62)	Peptidase dimerization domain
3	NADP-dependent isocitrate dehydrogenase *Pisum sativum*	gi|44921641	100 (13)	46258.6 (6.2)	Catalyses the reversible conversion of isocitrate to 2-oxoglutarate
4	Mercuric reductase, putative *Ricinus communis*	gi|255589011	99.829 (10)	48264.4 (7.15)	Pyridine nucleotide-disulphide oxidoreductase
5	Type 2 proly 4-hydroxylase *Nicotiana tabacum*	gi|215490183	86.137 (8)	36522.9 (6.64)	Oxygenization of peptidyl proline
6	Wound-responsive protein-related *Arabidopsis thaliana*	gi|15237744	87.926 (10)	44928.5 (6.97)	Nucleoside-diphosphate-sugar epimerases (cell-envelope biogenesis, outer membrane/carbohydrate transport and metabolism)
7	Putative aldo/keto reductase *Oryza sativa* (ISS. *Ostreococcus tauri*	gi|116059968	88.988 (8)	32271.8 (8.32)	Reduces aldehydes and ketones to primary and secondary alcohols
8	Alcohol dehydrogenase 1 *Petunia* × *hybrida*	gi|113363	86.452 (9)	42288.1 (6.19)	Responsible for the conversion of alcohols to aldehydes in plants and is important for NAD metabolism during anaerobic respiration
9	Os04g0244400 *Oryza sativa* Japonica group	gi|115457404	78.528 (8)	35479 (7.74)	Glutathione *S*-transferase
10	GBSSI *Iochroma edule*	gi|83755379	91.452 (8)	28328.2 (7.59)	Glycosyltransferase GTB type
11	Putative vitamin B-12-independent methionine synthase *Pisum sativum*	gi|121053772	100 (3)	34651.4 (5.75)	URO-D CIMS-like protein superfamily
12	ANN6 (ANNEXIN *Arabidopsis* 6. *A. thaliana*	gi|15238094	94.086 (10)	36661.1 (7.72)	Calcium ion-binding/calcium-dependent phospholipid binding
13	Peroxidase *Pisum sativum*	gi|62909963	100 (6)	38649.4 (8)	Horseradish peroxidase and related secretory plant peroxidases
14	Fructose-bisphosphate aldolase, cytoplasmic isozyme 2 *Pisum sativum*	gi|1168410	100 (11)	38638.1 (6.77)	Carbohydrate degradation, glycolysis
15	Endochitinase A2; Flags: Precursor *Pisum sativum*	gi|1705807	99.448 (3)	35738.8 (7.33))	Catalyses the hydrolysis of the beta-1,4-N-acetyl-D-glucosamine linkages in chitin polymers
16	Predicted protein *Populus trichocarpa*	gi|224080749	100 (3)	35304.5 (8.06)	Chitinase

fractions obtained after LYTRAP affinity column chromatography which obtained a recombinant cytosolic NADP-ICDH protein of approximately 66.0 kDa which is in line with the expected molecular mass of the cytosolic ICDH protein (45.0 kDa) plus the Ly-tag (21.28 kDa) predicted theoretically. The fractions E3–E7 show an adequate purity grade for this protein, with a NADP-ICDH activity of 10.1 ± 0.3 µmol NADPH min^{-1} mg^{-1} protein for the pharmacological *in vitro* assay with $ONOO^-$, using the molecule SIN-1 as a peroxynitrite donor (Chaki *et al.*, 2009). Fig. 5B depicts the effect of $ONOO^-$'s inhibition of activity in a dose-dependent manner ranging from 65% with 0.1 mM SIN-1 to 100% with 5 mM SIN-1. The reliability of nitration by SIN-1 of the cytosolic NADP-ICDH was corroborated by immunoblot analysis of the purified protein using an antibody against NO_2-Tyr. Fig. 5C shows that the nitration grade of NADP-ICDH increased with the SIN-1 concentration.

Identification of the tyrosine nitration site in nitrated recombinant cytosolic NADP-ICDH

With the aim of identifying which of the 12 tyrosines present in the pea plant's cytosolic NADP-ICDH are targets of this post-translational modification, non-nitrated and peroxynitrite-treated recombinant NADP-ICDHs were subjected to trypsin digestion followed by MALDI-TOF/TOF mass spectrometry examination. Supplementary Table S1 shows the list of peptides scanned and those identified

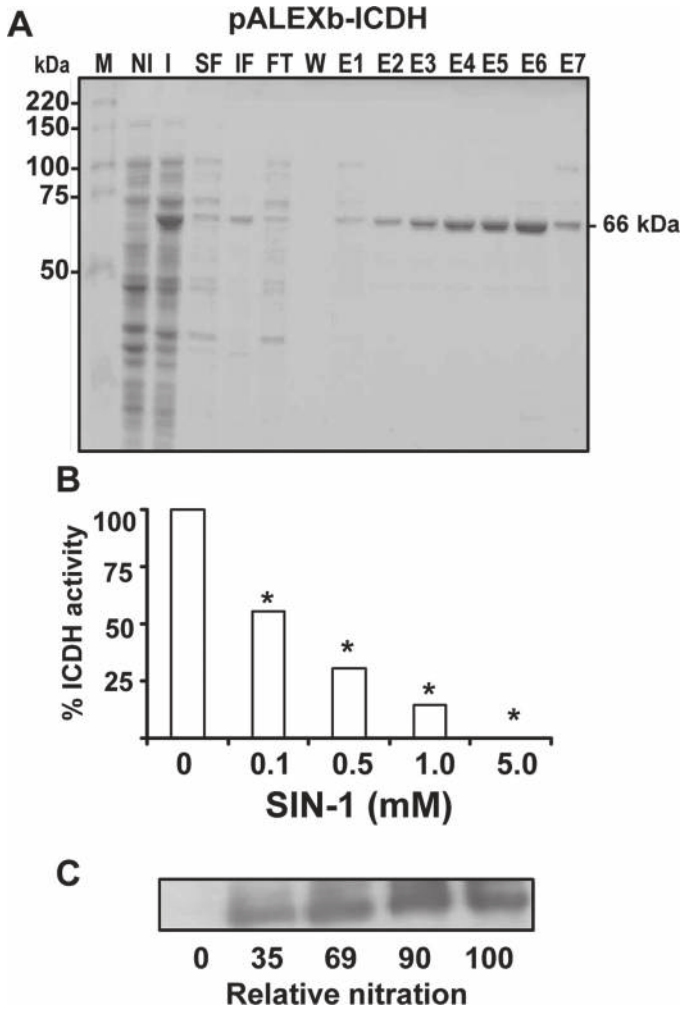

Fig. 5. Purification of recombinant cytosolic NADP-isocitrate dehydrogenase (ICDH) and effect of SIN-1 (peroxynitrite donor) on its activity. (A) SDS-PAGE analysis of the purification of the recombinant pea NADP-ICDH; Coomassie blue staining; E1–E7, elution fractions; FT, flow-through; I, total protein in induced culture; IF, insoluble fraction; M, molecular markers; NI, total protein in no-induced culture; SF, soluble fraction; W, wash. (B) Effect of SIN-1; purified NADP-ICDH was incubated with different concentrations of SIN-1 at 37 °C for 60 min. The specific activity of the recombinant peroxisomal NADP-ICDH was 10.1 ± 0.3 μmol NADPH min^{-1} mg^{-1} protein. Data are mean ± SEM of at least three replicates. Asterisks indicate significant differences from control values ($P < 0.05$). (C) Representative immunoblot showing the grade of tyrosine nitration of the cytosolic NADP-ICDH treated with different concentrations of SIN-1 and detected with an antibody against 3-nitrotyrosine (1:2500 dilution).

by LC-MS/MS. Among the identified peptides, only one contained a nitrated tyrosine with the amino acid sequence N389-EHYLNTEEFIDAVAAELK-C407.

Fig. 6 shows the comparison of the nitrated (top) and unmodified (bottom) MS/MS spectra of the identified peptide from the cytosolic NADP-ICDH. The nitrated peptide EHYLNTEEFIDAVAAELK ($Z = 2$) has a total of 18 amino acids and a mass of 2136 Da (2091 + 45 Da) which is compatible with the acquisition of a nitro group on Tyr392.

Fig. 7 shows the 3D model of cytosolic NADP-ICDH in pea plants showing Tyr392 and its potential interactions. Thus, Tyr392 is located at 8.6 Å of the Lys376 and His317 residues involved in the NADP-binding site (Huang and Colman, 2005). Arg111, Arg134, Tyr141, Lys214, Asp277, Asp281, and Glu306 appear to be the amino acids involved in isocitrate binding.

NADP-ICDH activity in roots of young and senescent pea plants

With the aim of investigating the physiological effects of the nitration of NADP-ICDH during senescence, its activity was analysed in the roots of young 8-day-old and senescent 71-day-old pea plants. Fig. 8 shows that NADP-ICDH activity fell by 75% in senescent roots. Catalase activity was also analysed and was observed to increase by 20%.

Discussion

In animal and plant cells, tyrosine nitration of proteins is a PTM mediated by NO-derived molecules that has been used as a marker of pathological processes and/or oxidative stress situations (Ischiropoulos, 2003; Dalle-Donne *et al.*, 2005; Corpas *et al.*, 2007). However, a body of new evidence indicates that tyrosine nitration could be involved in signalling processes (Gow *et al.*, 2004) and alter the protein function (Alvarez and Radi, 2003; Radi, 2004; Lozano-Juste *et al.*, 2011; Melo *et al.*, 2011). As far as is known, there is no information available on protein tyrosine nitration in relation to plant development and senescence. In order to obtain basic information on tyrosine nitration in plant proteins, this modification in the main organs of plants during their development and senescence has been analysed using a proteomic approach with an antibody against nitrotyrosine (Chaki *et al.*, 2009) which recognizes nitrated proteins that have undergone PTM mediated by NO-derived molecules. In this context, pea plants were selected as a model because basic information is available on the metabolism of NO (Leshem and Haramaty, 1996) which includes the characterization of L-arginine nitric oxide synthase (NOS) activity in different organs during seedling development and how NOS activity decreases in senescent leaves. Thus, various approaches have shown the presence of NOS activity (Barroso *et al.*, 1999; Corpas *et al.*, 2004) as well as the localization of NO in different organs of pea plants during their development (Corpas *et al.*, 2006a; Kolbert *et al.*, 2008) and the metabolism of RNS under environmental stress conditions (Barroso *et al.*, 2006; Rodríguez-Serrano *et al.*, 2006; Corpas *et al.*, 2008).

The data indicate that, during the development of pea plants, each organ has a specific nitration pattern. However, among the different organs analysed, the root particularly showed a pattern that clearly increased during both development and senescence. This organ was therefore chosen in

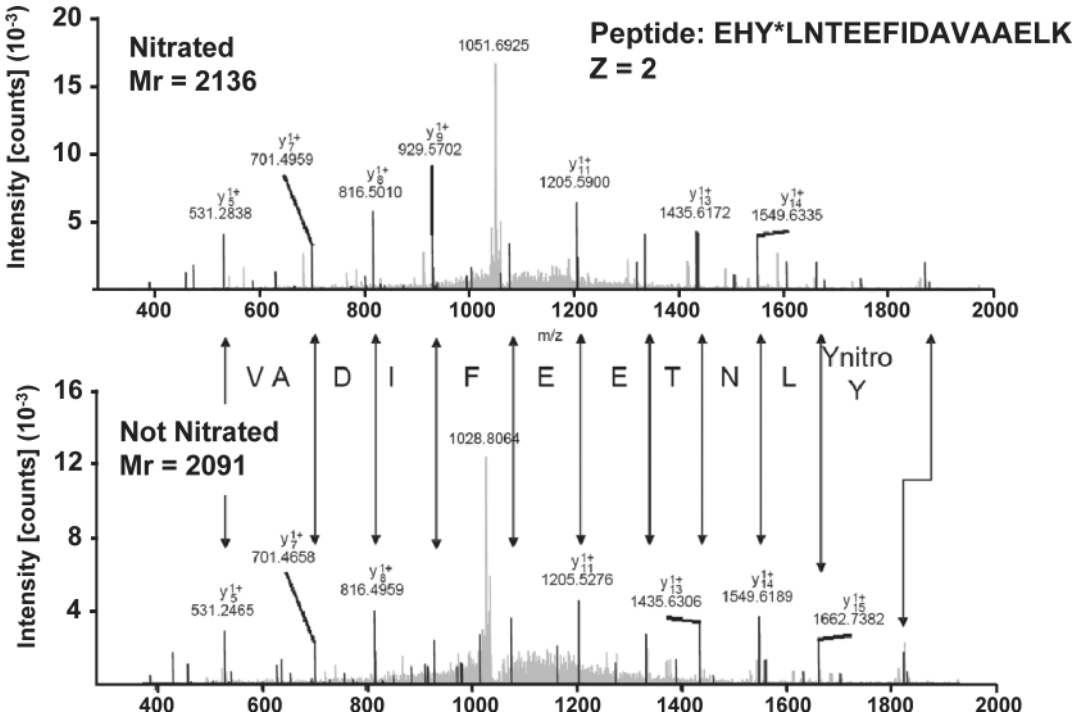

Fig. 6. Comparison of the nitrated (top) and unmodified (bottom) MS/MS spectra of the identified peptide (EHYLNTEEFIDAVAAELK) from the cytosolic pea NADP-isocitrate dehydrogenase.

order to gain a deeper understanding of the role played by nitration in roots.

Roots are essential organs that undergo morphological changes during plant development such as elongation and

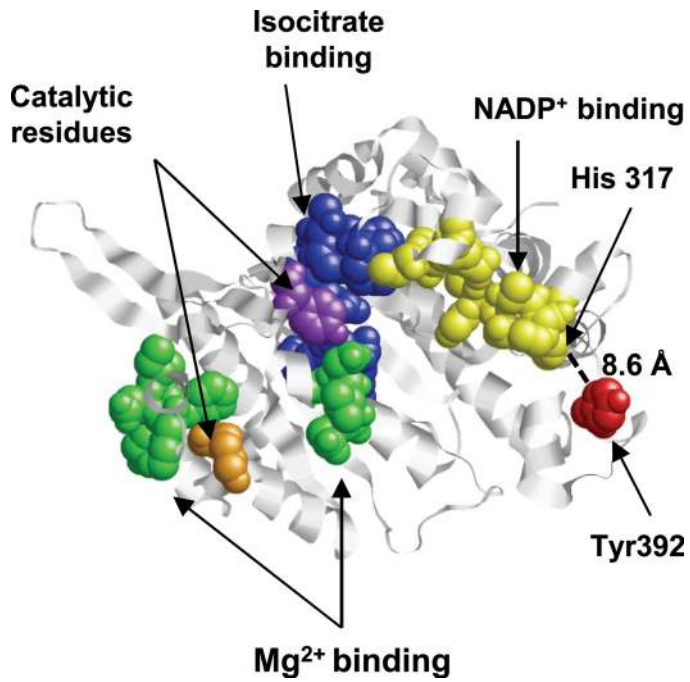

Fig. 7. Three-dimensional model of cytosolic NADP-isocitrate dehydrogenase showing Tyr392 (red) and its potential interactions. Conserved residues implicated in the binding of Mg^{2+} (green), isocitrate (blue), and NADP (yellow); catalytic residues are shown as purple or orange. The NADP-binding site includes Lys376 and His317 and is at 8.6 Å of the nitrated Tyr392 (this figure is available in colour at *JXB* online).

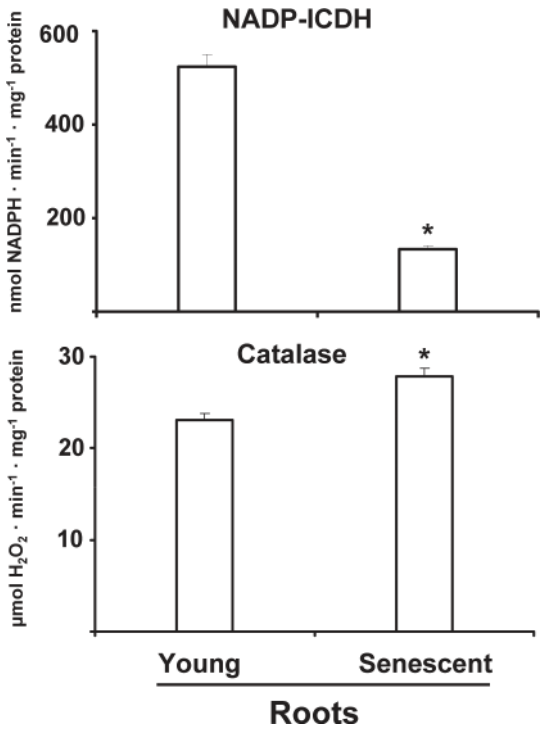

Fig. 8. NADP-isocitrate dehydrogenase and catalase activities in roots of young (8-day-old) and senescent (71-day-old) pea plants. Asterisks indicate significant differences from control values ($P < 0.05$)

the formation of secondary roots and hair roots to facilitate water and nutrient uptake and to anchor the plant body in the soil. In addition, under adverse growth conditions, root systems can also be subject to various changes in their architecture for adaptation purposes (de Dorlodot *et al.*, 2007). Roots also undergo structural and functional modifications in order to adapt to nutrient- and water-deficient stresses as well as to pathogen attacks and interaction with beneficial micro-organisms (fungus or bacteria) (Barea *et al.*, 2005; Mehta *et al.*, 2008). All these heterogeneous events change during root development and some can result in the senescence or death of certain roots or the whole root system. Various aspects of NO's role in root development have been studied that highlight its importance in roots. Thus, in pea plants, it has been demonstrated that there is a temporal correlation between root development and NO production from L-Arg-dependent NOS activity (Corpas *et al.*, 2006a). Additionally, the presence of NOS activity in plant roots has been detected in several plant species (Cueto *et al.*, 1996; Ribeiro *et al.*, 1999). Moreover, the application of exogenous NO donors induces root tip elongation (Kopyra and Gwózdz, 2003) and the formation of adventitious roots (Pagnussat *et al.*, 2002, 2004). Similar behaviour has been observed in tomato seedlings where the application of the NO donor sodium nitroprusside induced lateral root emergence and elongation, affecting the expression of cell cycle regulatory genes and modulated cellulose synthesis (Correa-Aragunde *et al.*, 2004, 2006, 2008). It has also been reported that NO donors counteract the inhibitory effect of heavy metals and salinity on root growth, suggesting that NO detected in the root hairs of pea plants could also play a protective role under abiotic stress conditions produced by heavy metals (Cd, Pb) and NaCl (Kopyra and Gwózdz, 2003). Under cadmium stress conditions, endogenous NO content is thus reduced in roots (Rodríguez-Serrano *et al.*, 2006). In previous studies of pea plants, in senescent pea leaves, the current study group observed that NO content is reduced (Corpas *et al.*, 2004), which was closely in line with previous data on pea and other plant species (Leshem and Haramaty, 1996; Leshem *et al.*, 1998). However, in roots from senescent plants, an opposite behaviour pattern was observed, with a rise in NO content being recorded. Moreover, oxidative stress has been reported in previous studies carried out during and induced senescence of pea leaves (Pastori and del Río, 1997). Under the experimental conditions of the current study group, the activity and protein expression of all SOD isoenzymes were observed to increase, indicating an alteration in the ROS metabolism (Swanson and Gilroy, 2010). This was accompanied by a rise in peroxynitrite and tyrosine nitration as evaluated by CLSM. Unfortunately, as far as is known, there is no data available on protein tyrosine nitration during development and senescence in plant cells in order to make a comparative analysis.

In recent years, the use of proteomic analysis has started to contribute to the identification of new targets of NO-mediated PTMs, and the application of exogenous RNS (NO donors, peroxynitrite) could help to identify these target proteins. However, the identification of targets under physiological conditions is a challenge where different factors must be considered such as the relatively low abundance of tyrosine nitration and that this nitration process is generally induced under adverse stress conditions. Therefore, the results of this study of roots contribute to the knowledge of tyrosine nitration as some of the candidates identified are involved in the process of microbial interaction as well as the response to biotic and abiotic stresses (Table 1) where tyrosine residues play an essential role. For example, chitinases catalyse the hydrolysis of chitin, which is a major component of the cell wall of most fungi, and it has been shown that some chitanase isoforms can mediate the formation of mycorrhiza (Slezack *et al.*, 2001) where NO accumulation has been described as a novel component in the signaling pathway that leads to the establishment of mycorrhizal symbiosis (Calcagno *et al.*, 2012). Furthermore, the catalytic site of this enzyme involves an essential tyrosine residue (Verburg *et al.*, 1992). Mercuric reductase is an inducible NADPH-dependent and flavin-containing disulphide oxidoreductase enzyme involved in environmental inorganic mercury detoxification. A putative mercuric reductase has been found in *Ricinus comunnis* (Chan *et al.*, 2010) and, under the experimental conditions of the current study group, also detected in pea roots. A remarkable feature of this enzyme is the binding site for Hg^{2+} involving two tyrosine residues (Rennex *et al.*, 1994). Fructose-bisphosphate aldolase (also called aldolase) is involved in carbohydrate degradation. This enzyme accumulates in roots, especially in the apical region. Aldolase has also been shown to be physically associated with vacuolar H-ATPase in roots and may regulate the vacuolar H-ATPase-mediated control of cell elongation that determines root length (Konishi *et al.*, 2004). In mammalian systems, this enzyme is subject to tyrosine nitration under different inflammatory conditions which causes activity loss (Koeck *et al.*, 2004). However, the possible involvement of tyrosine nitration in each protein needs to be corroborated experimentally.

The present study aimed to extend knowledge of the nitration process during plant development and senescence and so have focused on the cytosolic NADP-dependent isocitrate dehydrogenase (NADP-ICDH). This enzyme catalyses the oxidative decarboxylation of isocitrate to 2-oxoglutarate with the production of the reduced coenzyme NADPH (Gálvez and Gadal, 1995). Nitration has been shown to provoke a loss of function with respect to different plant activities *in vitro* condition such as ascorbate peroxidase, catalase (Clark *et al.*, 2000), *S*-Adenosyl homocysteine hydrolase (Chaki *et al.*, 2009), ferredoxin-NADP reductase, carbonic anhydrase (Chaki *et al.*, 2013), and *O*-acetylserine(thiol)lyase A1 (Álvarez *et al.*, 2011). Thus, mass spectrometric identification of Tyr392 as nitrated tyrosine residues in NADP-ICDH after treatment with SIN-1 offers an effective means of gaining a greater insight into the modulation of the enzyme by tyrosine nitration. According to the enzyme's model, Tyr392 is located at the active site, and nitration may account for the inhibition of enzymic activity. From a functional point of view, the location of Tyr392 suggests that its nitration may disrupt ICDH–coenzyme interaction and influence the enzyme's catalytic activity.

The presence of NADP-ICDH in roots has been described in many plant species including pea plants (Chen *et al.*, 1988),

alfalfa (Shorrosh and Dixon, 1992), soybean (Udvardi *et al.*, 1993), pines (Palomo *et al.*, 1998; Pascual *et al.*, 2008), and *Arabidopsis* (Leterrier *et al.*, 2012b) and it has always been associated with the metabolism of amino acids and ammonia (Fieuw *et al.*, 1995; Gálvez and Gadal, 1995). However, the concomitant generation of NADPH opens up new avenues in the functioning of this enzyme given that this cofactor is necessary for different metabolic pathways including the ascorbate–glutathione cycle, the superoxide radical generated by NADPH oxidase, and NO generation through L-arginine-dependent NOS activity. It has been suggested that this enzyme could support antioxidative systems in response to adverse stress conditions (Valderrama *et al.*, 2006; Leterrier *et al.*, 2007, 2012c; Airaki *et al.*, 2012) during leaf senescence (Corpas *et al.*, 1999), development and ripening of fruit (Gallardo *et al.*, 1995; Sadka *et al.*, 2000; Mateos *et al.*, 2009), and protection against oxidative stress in pea nodules (Marino *et al.*, 2007). Under the current experimental conditions, roots were observed during senescence to undergo a general increase in the content of NO, $ONOO^-$, and protein nitration. This was accompanied by an increase in antioxidative enzymes (SODs and catalase); however, NADP-ICDH activity was downregulated, which closely correlates with the inhibition provoked by the nitration of Tyr392. Similar behaviour has been observed in *Arabidopsis* plants subject to arsenic stress which, in roots, provoked a rise in the content of NO, superoxide radicals, $ONOO^-$, and protein nitration, although NADP-ICDH activity was observed to fall (Leterrier *et al.*, 2012a).

In summary, the data indicate that each organ has a specific nitrotyrosine protein pattern and that the intensity of the proteins which undergo this post-translation modification increases during the senescence of roots, stems, and leaves, with roots having the largest number of nitrated proteins. The nitrated proteins identified open up new perspectives where nitration of tyrosine could participate in regulating these proteins not only during development but also in the interaction of beneficial micro-organisms with roots (mycorrhizas, nodules) as well as responding to biotic and abiotic stresses. Specifically, during root senescence, cytosolic NADP-ICDH experiences specific nitration in Tyr392 that is involved in the binding site of NADP, which provokes its inhibition. Thus, it is proposed that the inhibition of NADP-ICDH should contribute to the process of root senescence given that this enzyme is involved in the nitrogen metabolism and generates NADPH which is a key cofactor in cellular redox homeostasis.

Supplementary material

Supplementary data are available at *JXB* online.

Supplementary Table S1. Peptides scanned and peptides identified by LC MS/MS.

Acknowledgements

JCBM acknowledges a Ph.D. fellowship (F.P.I.) from the Ministry of Science and Innovation. ML acknowledges a JAE-Doc contract from CSIC. This work was supported by ERDF-cofinanced grants from the Ministry of Science and Innovation (BIO2009–12003-C02-01 and BIO2009-12003-C02-02) and Junta de Andalucía (groups BIO192 and BIO 286). Microscopy analyses were carried out at the Technical Services of the University of Jaén. LC/MS/MS analyses were carried out at "Laboratorio de Proteómica" LP-CSIC/UAB, a member of ProteoRed network. Special thanks are given to Mr Carmelo Ruíz-Torres for his excellent technical support. Proteomic analysis was done at the Proteomic Service at University of Córdoba.

References

Aebi H. 1984. Catalase *in vitro*. *Methods in Enzymology* **105,** 121–126.

Airaki M, Leterrier M, Mateos RM, Valderrama R, Chaki M, Barroso JB, del Río LA, Palma JM, Corpas FJ. 2012. Metabolism of reactive oxygen species and reactive nitrogen species in pepper (*Capsicum annuum* L.) plants under low temperature stress. *Plant, Cell and Environment* **35,** 281–295.

Álvarez C, Lozano-Juste J, Romero LC, García I, Gotor C, León J. 2011. Inhibition of *Arabidopsis O*-acetylserine(thiol)lyase A1 by tyrosine nitration. *Journal of Biological Chemisty* **286,** 578–586.

Alvarez B, Radi R. 2003. Peroxynitrite reactivity with amino acids and proteins. *Amino Acids* **25,** 295–311.

Barea JM, Pozo MJ, Azcón R, Azcón-Aguilar C. 2005. Microbial co-operation in the rhizosphere. *Journal of Experimental Botany* **56,** 1761–1778.

Barroso JB, Corpas FJ, Carreras A, Sandalio LM, Valderrama R, Palma JM, Lupiáñez JA, del Río LA. 1999. Localization of nitric oxide synthase in plant peroxisomes. *Journal of Biological Chemisty* **274,** 36729–36733.

Barroso JB, Corpas FJ, Carreras A, *et al.* 2006. Localization of *S*-nitrosoglutathione and expression of *S*-nitrosoglutathione reductase in pea plants under cadmium stress. *Journal of Experimental Botany* **57,** 1785–1793.

Beauchamp C, Fridovich I. 1971. Superoxide dismutase: improved assays and an assay applicable to acrylamide gels. *Analytical Biochemistry* **44,** 276–287.

Calcagno C, Novero M, Genre A, Bonfante P, Lanfranco L. 2012. The exudate from an arbuscular mycorrhizal fungus induces nitric oxide accumulation in *Medicago truncatula* roots. *Mycorrhiza* **22,** 259–269.

Chaki M, Carreras A, López-Jaramillo J, Begara-Morales JC, Sánchez-Calvo B, Valderrama R, Corpas FJ, Barroso JB. 2013. Tyrosine nitration provokes inhibition of carbonic anhydrase (β-CA) activity under high temperature stress. *Nitric Oxide: Biology and Chemistry* 29C:30–33.

Chaki M, Valderrama R, Fernández-Ocaña AM, *et al.* 2009. Protein targets of tyrosine nitration in sunflower (*Helianthus annuus* L.) hypocotyls. *Journal of Experimental Botany* **60,** 4221–4234.

Chaki M, Valderrama R, Fernández-Ocaña AM, *et al.* 2011. High temperature triggers the metabolism of S-nitrosothiols in sunflower mediating a process of nitrosative stress which provokes the inhibition of ferredoxin-NADP reductase by tyrosine nitration. *Plant, Cell and Environment* **34,** 1803–1818.

Ceccarelli C, Grodsky NB, Ariyaratne N, Colman RF, Bahnson BJ. 2002. Crystal structure of porcine mitochondrial NADP-dependent isocitrate dehydrogenase complexed with Mn^{2+} and isocitrate. Insights into the enzyme mechanism. *Journal of Biological Chemisty* **277,** 43454–43462.

Chan AP, Crabtree J, Zhao Q, *et al.* 2010. Draft genome sequence of the oilseed species *Ricinus communis*. *Nature Biotechnology* **28,** 951–956.

Chen R, Le Maréchal P, Vidal J, Jacquot JP, Gadal P. 1988. Purification and comparative properties of the cytosolic isocitrate dehydrogenases (NADP) from pea (*Pisum sativum*) roots and green leaves. *European Journal of Biochemistry* **175,** 565–572.

Clark D, Durner J, Navarre DA, Klessig DF. 2000. Nitric oxide inhibition of tobacco catalase and ascorbate peroxidase. *Molecular Plant–Microbe Interacttions* **13,** 1380–1384.

Corpas FJ, Barroso JB, Carreras A, *et al.* 2004. Cellular and subcellular localization of endogenous nitric oxide in young and senescent pea plants. *Plant Physiology* **136,** 2722–2733.

Corpas FJ, Barroso JB, Carreras A, Valderrama R, Palma JM, León AM, Sandalio LM, del Río LA. 2006a. Constitutive arginine-dependent nitric oxide synthase activity in different organs of pea seedlings during plant development. *Planta* **224,** 246–254.

Corpas FJ, Barroso JB, Sandalio LM, Palma JM, Lupiáñez JA, del Rio LA. 1999. Peroxisomal NADP-dependent isocitrate dehydrogenase. Characterization and activity regulation during natural senescence. *Plant Physiology* **121,** 921–928.

Corpas FJ, Chaki M, Fernández-Ocaña A, Valderrama R, Palma JM, Carreras A, Begara-Morales JC, Airaki M, del Río LA, Barroso JB. 2008. Metabolism of reactive nitrogen species in pea plants under abiotic stress conditions. *Plant Cell Physiology* **49,** 1711–1722.

Corpas FJ, del Río LA, Barroso JB. 2007. Need of biomarkers of nitrosative stress in plants. *Trends in Plant Sciences* **12,** 436–438.

Corpas FJ, Fernández-Ocaña A, Carreras A, *et al.* 2006b. The expression of different superoxide dismutase forms is cell-type dependent in olive (*Olea europaea* L.) leaves. *Plant Cell Physiology* **47,** 984–994.

Corpas FJ, Hayashi M, Mano S, Nishimura M, Barroso JB. 2009. Peroxisomes are required for in vivo nitric oxide accumulation in the cytosol following salinity stress of *Arabidopsis* plants. *Plant Physiology* **151,** 2083–2094.

Corpas FJ, Palma JM, del Río LA, Juan B, Barroso JB. 2013. Protein tyrosine nitration in higher plants grown under natural and stress conditions. *Frontiers in Plant Proteomics* (in press).

Corpas FJ, Sandalio LM, del Río LA, Trelease RN. 1998. Copper-zinc superoxide dismutase is a constituent enzyme of the matrix of peroxisomes in the cotyledons of oilseed plants. *New Phytologist* **138,** 307–314.

Corpas FJ, Trelease RT. 1998. Differential expression of ascorbate peroxidase and a putative molecular chaperone in the boundary membrane of differentiating cucumber seedling peroxisomes. *Journal of Plant Physiology* **153,** 332–338.

Correa-Aragunde N, Graziano M, Chevalier C, Lamattina L. 2006. Nitric oxide modulates the expression of cell cycle regulatory genes during lateral root formation in tomato. *Journal of Experimental Botany* **57,** 581–588.

Correa-Aragunde N, Graziano M, Lamattina L. 2004. Nitric oxide plays a central role in determining lateral root development in tomato. *Planta* **218,** 900–905.

Correa-Aragunde N, Lombardo C, Lamattina L. 2008. Nitric oxide: an active nitrogen molecule that modulates cellulose synthesis in tomato roots. *New Phytologist* **179,** 386–396.

Cueto M, Hernández-Perea O, Martín R, Ventura ML, Rodrigo J, Lamas S, Golvano MP. 1996. Presence of nitric oxide synthase activity in roots and nodules of Lupinus albus. *FEBS Letters* **398,** 159–164.

Dalle-Donne I, Scaloni A, Giustarini D, Cavarra E, Tell G, Lungarella G, Colombo R, Rossi R, Milzani A. 2005. Proteins as biomarkers of oxidative/nitrosative stress in diseases: the contribution of redox proteomics. *Mass Spectrometry Reviews* **24,** 55–99.

de Dorlodot S, Forster B, Pagès L, Price A, Tuberosa R, Draye X. 2007. Root system architecture: opportunities and constraints for genetic improvement of crops. *Trends in Plant Sciences* **12,** 474–481.

Daiber A, Bachschmid M, Beckman JS, Munzel T, Ullrich V. 2004. The impact of metal catalysis on protein tyrosine nitration by peroxynitrite. *Biochemical and Biophysical Research Communications* **317,** 873–381.

Eiserich JP, Estevez AG, Bamberg TV, Ye YZ, Chumley PH, Beckman JS, Freeman BA. 1999. Microtubule dysfunction by posttranslational nitrotyrosination of alpha-tubulin: a nitric oxide-dependent mechanism of cellular injury. *Proceedings of the National Academy of Sciences, USA* **96,** 6365–6370.

Fieuw S, Müller-Röber B, Gálvez S, Willmitzer L. 1995. Cloning and expression analysis of the cytosolic NADP-dependent isocitrate dehydrogenase from potato. Implications for nitrogen metabolism. *Plant Physiology* **107,** 905–913.

Gálvez S, Gadal P. 1995. On the function of the NADP-dependent isocitrate dehydrogenase isoenzymes in living organisms. *Plant Science* **105,** 1–14.

Gallardo F, Gálvez S, Gadal P, Cánovas FM. 1995. Changes in NADP-linked isocitrate dehydrogenase during tomato fruit ripening. Characterization of the predominant cytosolic enzyme from green and ripe pericarp. *Planta* **196,** 148–154.

Gow AJ, Farkouh CR, Munson DA, Posencheg MA, Ischiropoulos H. 2004. Biological significance of nitric oxide-mediated protein modifications. *American Journal of Physiology. Lung Cellular and Molecular Physiology* **287,** L262–L268.

Greenacre SA, Ischiropoulos H. 2001. Tyrosine nitration: localisation, quantification, consequences for protein function and signal transduction. *Free Radical Research* **34,** 541–581.

Huang YC, Colman RF. 2005. Location of the coenzyme binding site in the porcine mitochondrial NADP-dependent isocitrate dehydrogenase. *Journal of Biological Chemisty* **280,** 30349–30353.

Ischiropoulos H. 2003. Biological selectivity and functional aspects of protein tyrosine nitration. *Biochemical and Biophysical Research Communications* **305,** 776–783.

Ischiropoulos H, Gow A. 2005. Pathophysiological functions of nitric oxide-mediated protein modifications. *Toxicology* **208,** 299–303.

Kanematsu S, Asada K. 1989. CuZn-superoxide dismutases from the fern *Equisetum arvense* and the green alga *Spirogyra* sp.:

occurrence of chloroplast and cytosol types of enzyme. *Plant Cell Physiology* **30,** 717–727.

Koeck T, Levison B, Hazen SL, Crabb JW, Stuehr DJ, Aulak KS. 2004. Tyrosine nitration impairs mammalian aldolase A activity. *Molecular Cell Proteomics* **3,** 548–557.

Kolbert Z, Bartha B, Erdei L. 2008. Osmotic stress- and indole-3-butyric acid-induced NO generation are partially distinct processes in root growth and development in *Pisum sativum*. *Physiologica Plantarum* **133,** 406–416.

Konishi H, Yamane H, Maeshima M, Komatsu S. 2004. Characterization of fructose-bisphosphate aldolase regulated by gibberellin in roots of rice seedling. *Plant Molecular Biology* **56,** 839–848.

Kopyra M, Gwózdz EA. 2003. Nitric oxide stimulates seed germination and counteracts the inhibitory effect of heavy metals and salinity on root growth of *Lupinus luteus*. *Plant Physiology and Biochemistry* **41,** 1011–1017.

Laemmli UK. 1970. Cleavage of structural proteins during the assembly of the head of bacteriophage T4. *Nature* **227,** 680–685.

Leshem YY, Haramaty E. 1996. The characterization and contrasting effects of the nitric oxide free radical in vegetative stress and senescence of *Pisum sativum* Linn. foliage. *Journal of Plant Physiology* **148,** 258–263.

Leshem YY, Wills RBH, Veng-Va Ku V. 1998. Evidence for the function of the free radical gas-nitric oxide (NO) as an endogenous maturation and senescence regulating factor in higher plants. *Plant Physiology and Biochemistry* **36,** 825–833.

Leterrier M, Airaki M, Palma JM, Chaki M, Barroso JB, Corpas FJ. 2012a. Arsenic triggers the nitric oxide (NO) and *S*-nitrosoglutathione (GSNO) metabolism in *Arabidopsis*. *Environmental Pollution* **166,** 136–143.

Leterrier M, Barroso JB, Palma JM, Corpas FJ. 2012b. Cytosolic NADP-isocitrate dehydrogenase in *Arabidopsis* leaves and roots. *Biologia Plantarum* **56,** 705–710.

Leterrier M, Barroso JB, Valderrama R, Palma JM, Corpas FJ. 2012c. NADP-dependent isocitrate dehydrogenase (NADP-ICDH) from *Arabidopsis* roots contributes in the mechanism of defence against the nitro-oxidative stress induced by salinity. *Scientific World Journal* **2012,** 694740.

Leterrier M, del Río LA, Corpas FJ. 2007. Cytosolic NADP-isocitrate dehydrogenase of pea plants: genomic clone characterization and functional analysis under abiotic stress conditions. *Free Radical Research* **41,** 191–199.

Lozano-Juste J, Colom-Moreno R, León J. 2011. *In vivo* protein tyrosine nitration in *Arabidopsis thaliana*. *Journal of Experimental Botany* **62,** 3501–3517.

Marino D, González EM, Frendo P, Puppo A, Arrese-Igor C. 2007. NADPH recycling systems in oxidative stressed pea nodules: a key role for the NADP+-dependent isocitrate dehydrogenase. *Planta* **225,** 413–421.

Mateos RM, Bonilla-Valverde D, del Río LA, Palma JM, Corpas FJ. 2009. NADP-dehydrogenases from pepper fruits: effect of maturation. *Physiologica Plantarum* **135,** 130–139.

Mehta A, Magalhães BS, Souza DS, Vasconcelos EA, Silva LP, Grossi-de-Sa MF, Franco OL, da Costa PH, Rocha TL. 2008. Rooteomics: the challenge of discovering plant defense-related proteins in roots. *Current Protein and Peptide Science* **9,** 108–116.

Melo PM, Silva LS, Ribeiro I, Seabra AR, Carvalho HG. 2011. Glutamine synthetase is a molecular target of nitric oxide in root nodules of *Medicago truncatula* and is regulated by tyrosine nitration. *Plant Physiology* **157,** 1505–1517.

Pagnussat GC, Lanteri ML, Lombardo MC, Lamattina L. 2004. Nitric oxide mediates the indole acetic acid induction activation of a mitogen-activated protein kinase cascade involved in adventitious root development. *Plant Physiology* **135,** 279–286.

Pagnussat GC, Simontacchi M, Puntarulo S, Lamattina L. 2002. Nitric oxide is required for root organogenesis. *Plant Physiology* **129,** 954–956.

Palomo J, Gallardo F, Suarez MF, Canovas FM. 1998. Purification and characterization of NADP+-linked isocitrate dehydrogenase from scots pine. Evidence for different physiological roles of the enzyme in primary development. *Plant Physiology* **118,** 617–626.

Pascual MB, Molina-Rueda JJ, Cánovas FM, Gallardo F. 2008. Spatial distribution of cytosolic NADP-isocitrate dehydrogenase in pine embryos and seedlings. *Tree Physiology* **28,** 1773–1782.

Pastori GM, del Río LA. 1997. Natural senescence of pea leaves: an activated oxygen-mediated function for peroxisomes. *Plant Physiology* **113,** 411–418.

Perkins DN, Pappin DJ, Creasy DM, Cottrell JS. 1999. Probability based protein identification by searching sequence databases using mass spectrometry data. *Electrophoresis* **20,** 3551–3567.

Radi R. 2004. Nitric oxide, oxidants, and protein tyrosine nitration. *Proceedings of the National Academy of Sciences, USA* **101,** 4003–4008.

Rennex D, Pickett M, Bradley M. 1994. In vivo and in vitro effects of mutagenesis of active site tyrosine residues of mercuric reductase. *FEBS Letters* **355,** 220–222.

Ribeiro EA, Cunha FQ, Tamashiro WMSC, Martins IS. 1999. Growth phase-dependent subcellular localization of nitric oxide synthase in maize cells. *FEBS Letters* **445,** 283–286.

Rodríguez-Serrano M, Romero-Puertas MC, Zabalza A, Corpas FJ, Gómez M, del Río LA, Sandalio LM. 2006. Cadmium effect on oxidative metabolism of pea (*Pisum sativum* L.) roots. Imaging of reactive oxygen species and nitric oxide accumulation in vivo. *Plant, Cell and Environment* **29,** 1532–44.

Sadka A, Dahan E, Or E, Cohen L. 2000. NADP-isocitrate dehydrogenase gene expression and isozyme activity during citrus fruit development. *Plant Science* **158,** 173–181.

Slezack S, Negrel J, Bestel-Corre G, Dumas-Gaudot E, Gianinazzi S. 2001. Purification and partial amino acid sequencing of a mycorrhiza-related chitinase isoform from *Glomus mosseae*-inoculated roots of *Pisum sativum* L. *Planta* **213,** 781–787.

Shorrosh BS, Dixon RA. 1992. Molecular characterization and expression of an isocitrate dehydrogenase from alfalfa (*Medicago sativa* L.) *Plant Molecular Biology* **20,** 801–807.

Swanson S, Gilroy S. 2010. ROS in plant development. *Physiologica Plantarum* **138,** 384–392.

Tanou G, Filippou P, Belghazi M, Job D, Diamantidis G, Fotopoulos V, Molassiotis A. 2012. Oxidative and nitrosative-based

signaling and associated post-translational modifications orchestrate the acclimation of citrus plants to salinity stress. *The Plant Journal* **72,** 585–599.

Udvardi MK, McDermott TR, Kahn ML. 1993. Isolation and characterization of a cDNA-encoding NADP-specific isocitrate dehydrogenase from soybean (*Glycine max*.) *Plant Molecular Biology* **21,** 739–752.

Valderrama R, Corpas FJ, Carreras A, Fernández-Ocaña A, Chaki M, Luque F, Gómez-Rodríguez MV, Colmenero-Varea P, del Río LA, Barroso JB. 2007. Nitrosative stress in plants. *FEBS Letters* **581,** 453–461.

Valderrama R, Corpas FJ, Carreras A, Gómez-Rodríguez MV, Chaki M, Pedrajas JR, Fernández-Ocaña A, del Río LA, Barroso JB. 2006. The dehydrogenase-mediated recycling of NADPH is a key antioxidant system against salt-induced oxidative stress in olive plants. *Plant, Cell and Environment* **29,** 1449–1459.

Verburg JG, Smith CE, Lisek CA, Huynh QK. 1992. Identification of an essential tyrosine residue in the catalytic site of a chitinase isolated from *Zea mays* that is selectively modified during inactivation with 1-ethyl-3-(3-dimethylaminopropyl.-carbodiimide. *Journal of Biological Chemisty* **267,** 3886–3893.